3D printed PLGA implants: How the filling density affects drug release

C. Bassand, F. Siepmann, L. Benabed, J. Verin, J. Freitag, Sébastien Charlon, J. Soulestin, J. Siepmann

Research article

3D printed PLGA implants: How the filling density affects drug release

C. Bassand[1], F. Siepmann[1], L. Benabed[1], J. Verin[1], J. Freitag[1], S. Charlon[2], J. Soulestin[2], J. Siepmann[1]*

[1]*Univ. Lille, Inserm, CHU Lille, U1008, F-59000 Lille, France*
[2]*IMT Lille Douai, Dept Polymers & Composites Technol & Mech Engn, F-59500 Douai, France*

*correspondence:
Prof. Dr. Juergen SIEPMANN
College of Pharmacy, INSERM U1008
University of Lille, 3, rue du Professeur Laguesse, 59006 Lille, France
juergen.siepmann@univ-lille.fr

Abstract

Different types of ibuprofen-loaded, poly (D,L lactic-co-glycolic acid) (PLGA)-based implants were prepared by 3D printing (Droplet Deposition Modeling). The theoretical filling density of the mesh-shaped implants was varied from 10 to 100 %. Drug release was measured in agarose gels and in well agitated phosphate buffer pH 7.4. The key properties of the implants (and dynamic changes thereof upon exposure to the release media) were monitored using gravimetric measurements, optical microscopy, Differential Scanning Calorimetry, Gel Permeation Chromatography, and Scanning Electron Microscopy. Interestingly, drug release was similar for implants with 10 and 30 % filling density, irrespective of the experimental set-up. In contrast, implants with 100 % filling density showed slower release kinetics, and the shape of the release curve was altered in agarose gels. These observations could be explained by the existence (or absence) of a continuous aqueous phase between the polymeric filaments and the "orchestrating role" of substantial system swelling for the control of drug release. At lower filling densities, it is sufficient for the drug to be released from a *single filament*. In contrast, at high filling densities, the *ensemble of filaments* acts as a much larger (more or less homogeneous) polymeric matrix, and the average diffusion pathway to be overcome by the drug is much longer. Agarose gel (mimicking living tissue) hinders substantial PLGA swelling and delays the onset of the final rapid drug release phase. This improved mechanistic understanding of the control of drug release from PLGA-based 3D printed implants can help to facilitate the optimization of this type of advanced drug delivery systems.

Key words: PLGA; implant; 3D printing; ibuprofen; swelling; drug release mechanism

1. Introduction

Poly (D,L lactic-co-glycolic acid) (PLGA)-based drug delivery systems offer an interesting potential for controlled drug delivery applications [1,2,3,4,5], because they: (i) are completely biodegradable, (ii) are biocompatible [6], and (iii) can provide flexible release rates and periods [7,8,9,10]. A large variety of drugs has been incorporated into this type of drug delivery systems, including small and large molecules as well as freely and poorly water soluble compounds [11,12,13]. Different types of systems have been proposed and reached the market [14,15]: Pre-formed implants and microparticles as well as liquid formulations, which are injected into the patient's body and harden in vivo ("in-situ forming implants").

To adjust desired release kinetics for a given drug, various formulation and processing parameters can be varied. This includes for instance the drug content, type of PLGA (differing in the average polymer molecular weight, type of end groups and lactic acid: glycolic acid ratio), geometry and dimensions of the device, addition of further excipients as well as the manufacturing procedure. The impact of the latter is not to be underestimated, because it can strongly affect the resulting inner system structure, which can be of crucial importance for the conditions of drug release. For example, PLGA-based microparticles can be prepared via different solvent extraction/evaporation methods, using oil-in-water (O/W) emulsions or water-in-oil-in-water (W/O/W) emulsions [16,17]. In the first case, non-porous microparticles with relatively slow drug release can be obtained, whereas in the latter case highly porous systems can be prepared with much higher drug release rates (even if the qualitative and quantitative compositions of the microparticles are very similar): The presence of numerous inner pores can facilitate drug transport within the microparticles.

Despite the considerable practical importance of PLGA-based controlled drug delivery systems, the physico-chemical phenomena which are involved in the control of drug release are often not fully understood. This hampers the development of new drug products: Cost-intensive and time-consuming series of trial-and-error experiments are required, and unexpected tendencies can be observed. This can in great part be attributed to the complexity of the underlying drug release mechanisms [18,19,20,21,22,23]. Upon contact with aqueous media, water penetrates into the systems and rather rapidly wets the entire devices. This results in ester bond cleavage throughout the systems ("bulk degradation") [24]. If the drug is present in the form of particles (crystalline or amorphous), the latter dissolve in the water and the drug becomes mobile. Due to the concentration gradients, the dissolved drug subsequently diffuses out of the system. Depending on the initial loading and solubility of the drug in the wetted PLGA matrix, dissolved and non-dissolved drug might co-exist during considerable periods of time. Importantly, only dissolved drug is mobile and can diffuse out. This diffusional mass transport might occur through water-filled pores or channels and/or through an intact, more or less swollen polymeric network. The affinity of the drug to the PLGA and to water, as well as its molecular weight affect the importance of these different diffusion pathways. Certain drugs also act as plasticizers for PLGA, increasing the mobility of the macromolecular chains [25]. Furthermore, the hydrolytic cleavage of each ester bond generates a new -COOH end group. So, the pH within the drug delivery system might locally substantially drop [26,27,28,29], leading to autocatalytic effects: Ester bond cleavage is catalyzed by protons. Depending on the dimensions of the drug delivery systems, water-soluble generated acids can more or less rapidly diffuse out into the surrounding environment, so that the micro pH more or less drastically decreases. Accelerated polymer degradation leads to increased porosity and increased drug mobility. Certain systems have been reported to become highly porous at their center over time [16]. These dynamic changes in the system's structure upon exposure to the release medium can strongly affect drug mobility. In addition, polymer swelling has been suggested to play a key role for the control of drug release from PLGA-based implants and microparticles [30,31].

Different manufacturing techniques can be applied to prepare PLGA implants for controlled drug delivery, including for instance compression [32], casting [33], hot melt extrusion [34] and 3D printing [35,36]. The latter process offers the advantage to allow for personalized medication [37,38,39,40,41]: Depending on the specific needs of each patient (e.g. dosage, release rate, release period, combination of drugs), personalized implants can be printed. In addition, the implant's shape and geometry can be adapted to each patient. However, yet relatively little knowledge is available on the processability of PLGA-drug blends, the resulting drug release kinetics and the possibilities to adjust desired drug release kinetics. One of the simplest parameters which can be varied during implant printing is the "filling density" of the system: The implant can be designed as a non-porous device (100 % filling density), or as a highly porous system (e.g. 10 % filling density). However, so far it is unclear how drastically the filling density of the implant impacts the resulting drug release patterns.

The aim of this study was to better understand the importance of the filling density of 3D printed PLGA implants for the control of drug release. Ibuprofen, a small, acidic molecule with anti-inflammatory activity, was studied as the drug. An Arburg Plastic Freeforming (APF) printer was used to prepare different types of implants, which were thoroughly characterized before and after exposure to different release media in two experimental set-ups. The classical exposure to well agitated bulk fluid (phosphate buffer pH 7.4) was compared with the exposure to 0.5 % agarose gels: aiming to better mimic the presence of living tissue surrounding the implant in the patient's body [42,43,44]. In addition, gravimetric measurements, optical microscopy, Differential Scanning Calorimetry, Gel Permeation Chromatography, and Scanning Electron Microscopy were applied to better understand the underlying mass transport mechanisms in the different types of implants under the investigated conditions.

2. Materials and methods

2.1. Materials

Poly (D,L lactic-co-glycolic acid) (PLGA, 50:50 lactic acid: glycolic acid; Resomer RG 503H; Evonik, Darmstadt, Germany); ibuprofen (BASF, Ludwigshafen, Germany); agarose (genetic analysis grade) and tetrahydrofuran (HPLC grade) (Fisher Scientific, Illkirch, France); potassium dihydrogen orthophosphate and sodium hydroxide (Acros Organics, Geel, Belgium); acetonitrile (VWR, Fontenoy-sous-Bois, France); sodium hydrogen phosphate (Na_2HPO_4; Panreac Quimica, Barcelona, Spain).

2.2 Implant preparation

PLGA flakes were milled (4 x 30 s) in a grinder (Valentin, Seb, Ecully, France). Ibuprofen was used as received. Appropriate amounts of polymer and drug powders were manually blended for 5 min in a mortar with a pestle, followed by extrusion using a Nano 16 twin-screw extruder (screw diameter = 16 mm, length/diameter ratio = 26.25, gravitational feeder; Leistritz, Nuremberg, Germany), equipped with a 2 mm diameter die. The process temperatures were kept constant at 80 - 75 - 70 - 65 °C (die - zone 3 - zone 2 - zone 1). The screw speed was set to 50 rpm, the screw configuration is illustrated in Figure S1. After cooling to room temperature, the hot melt extrudates were manually cut into small cylinders of 5 mm length. The latter are called "pellets" in this article. They served as intermediate product and were fed into an Arburg Plastic Freeforming (APF) printer (Freeformer, Arburg, Germany) [45,46]. The nozzle diameter was 250 µm, the printing speed was set to 40 mm/s, the temperatures of the 1st, 2nd and 3rd heating zones were 120, 100 and 100 °C, respectively. The temperature of the printing chamber was 25 °C. The implants had the shape of parallelepiped meshes (10 × 10 × 2.5 mm), as illustrated in Figure 1. The theoretical filling density was set to 10, 30, or 100 %, respectively. The lower the filling density, the more important was the fraction of voids.

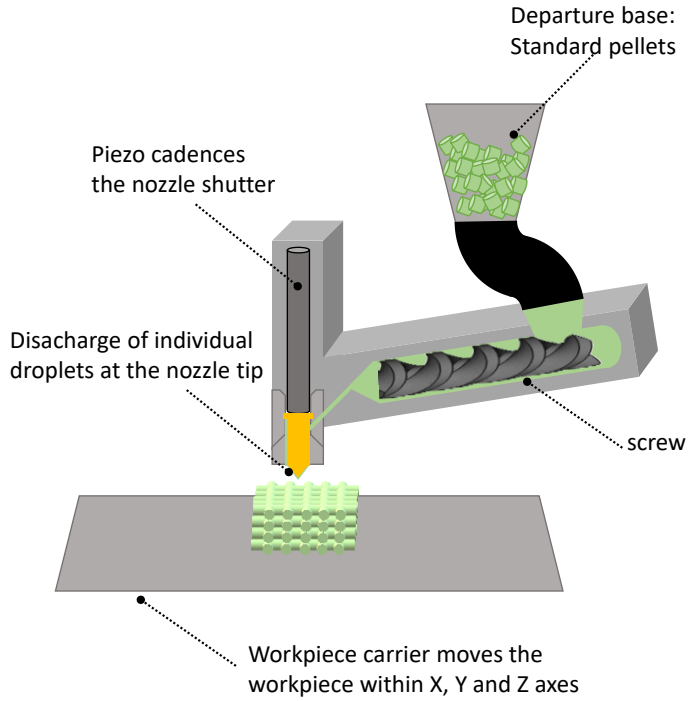

Figure 1: Schematic presentation of the applied 3D printing technique: Arburg Plastic Freeforming Droplet Deposition Modeling (APF DDM) (reprinted from [36], with permission).

2.3 Optical microscopy

Pictures of the implants before exposure to the release medium were taken using a SZN-6 trinocular stereo zoom microscope (Optika, Ponteranica, Italy), equipped with an optical camera (Optika Vison Lite 2.1 software). The dimensions of the meshes and pore sizes were determined using the ImageJ software (US National Institutes of Health, Bethesda, Maryland, USA). Mean values +/- standard deviations are reported (n = 36).

2.4 Practical drug loading

Pellets or pieces of 3D printed implants were dissolved in 5 mL acetonitrile, followed by filtration (PVDF syringe filters, 0.45 µm; Agilent Technologies, Santa Clara, USA). The drug content was measured by HPLC-UV analysis using a Thermo Fisher Scientific Ultimate 3000 Series apparatus, equipped with a LPG 3400 SD/RS pump, an auto sampler (WPS-3000 SL) and a UV-Vis detector (VWD-3400RS) (Thermo Fisher Scientific, Waltham, USA). A reversed phase column C18 (Gemini 5 µm; 110 A°; 150 x 4.6 mm; Phenomenex, Le Pecq, France) was used. The mobile phase was a mixture of 30 mM Na_2HPO_4 pH 7.0: acetonitrile (60:40, v:v). The detection wavelength was 225 nm, the flow rate was set to 0.5 mL/min. Ten microliter samples were injected. Mean values +/- standard deviations are reported (n = 6).

2.5 Differential scanning calorimetry (DSC)

DSC thermograms of the raw materials (PLGA and ibuprofen), pellets and 3D printed implants were recorded using a DCS1 Star System (Mettler Toledo, Greifensee, Switzerland). Approximately 5 mg samples were heated in pierced aluminum pans from -70 to 120 °C, followed by cooling to -70 °C, and re-heating to 120 °C (heating/cooling rate = 10 °C/min). The reported glass temperatures (Tgs) were determined from the 1st heating cycles in the case of the pellets and 3D printed implants (the thermal history being of interest). The Tgs of the PLGA raw material was determined from the 2nd heating cycle (the thermal history not being of interest). All experiments were conducted in triplicate. Mean values +/- standard deviations are reported.

2.6 Gel permeation chromatography (GPC)

The average polymer molecular weight (Mw) of the PLGA was determined by gel permeation chromatography (GPC) as follows: Samples were dissolved in tetrahydrofuran (3 mg/mL). Fifty µL samples were injected into an Alliance GPC apparatus (refractometer detector: 2414 RI, separation module e2695, Empower GPC software; Waters, Milford, USA), equipped with a PLgel 5 µm MIXED-D column (kept at 35°C, 7.8 × 300 mm; Agilent). Tetrahydrofuran was the mobile phase (flow rate: 1 mL/min). Polystyrene standards with molecular weights between 1,480 and 70,950 Da (Polymer Laboratories, Varian, Les Ulis, France) were used to prepare the calibration curve. All experiments were conducted in triplicate. Mean values +/- standard deviations are reported.

2.7 In vitro drug release

Two experimental set-ups were used to measure ibuprofen release from the PLGA implants:

In agarose gels

Implants were embedded in 10 mL agarose gel in 50 mL tubes (352070 Corning-Falcon, New York, USA), as illustrated in Figure 2A (1 implant per tube). The agarose gel was prepared as follows: An 0.5% (w:v) agarose dispersion in phosphate buffer pH 7.4 USP 42 was heated to 100 °C under magnetic stirring (250 rpm) until a clear solution was obtained. The latter was cooled to 47 °C and continuously stirred (to prevent gelation). Five mL of the solution was placed at the bottom of a tube and cooled in a refrigerator for 5 min to allow for gelation. An implant was carefully placed on top of the gel, and covered with second layer of 5 mL agarose solution (47 °C), followed by cooling in a refrigerator for 5 min. Forty mL phosphate buffer pH 7.4 were added on top of the gel, and the tube was placed in a horizontal shaker (80 rpm, 37 °C; GFL 3033, Gesellschaft fuer Labortechnik, Burgwedel, Germany). At predetermined time points, the entire bulk fluid was replaced by fresh (pre-heated) release medium. The withdrawn samples were filtered (PVDF syringe filter, 0.45 µm; Agilent, Santa Clara, California, USA) and analyzed for their ibuprofen contents by HPLC-UV, as described in *section 2.4*.

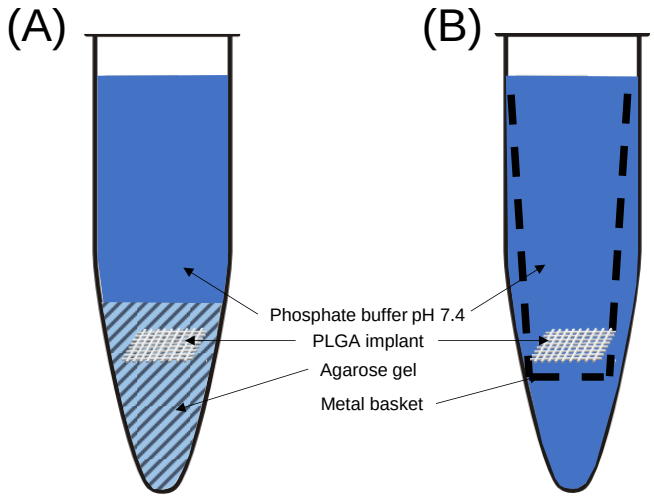

Figure 2: Schematic presentations of the experimental set-ups used to monitor drug release from the investigated PLGA-based implants. The tubes were kept at 37 ° and horizontally shaken at 80 rpm. A) Implants were embedded in agarose gels, which were exposed to phosphate buffer pH 7.4. B) Implants were directly exposed to phosphate buffer pH 7.4 (a metal basket avoiding sinking or sticking to the walls). In all cases, sink conditions were provided throughout the experiments in the well agitated bulk fluids.

In well agitated phosphate buffer pH 7.4

Implants were placed into 50 mL tubes (352070 Corning-Falcon), filled with 50 mL phosphate buffer pH 7.4 (1 implant per tube). A metal basket assured that the implants could not sink to the bottom of the tubes or stick to the latter's walls (Figure 2B), potentially altering the surface available for drug release. The tubes were placed in a horizontal shaker (80 rpm, 37°C; GFL 3033). At predetermined time points, the entire bulk fluid was replaced by fresh release medium. The withdrawn samples were treated as in the case of drug release measurements in agarose gels.

In all cases, sink conditions were provided throughout the experiments in the agitated bulk fluids. All experiments were conducted in triplicate. Mean values +/- standard deviations are reported.

2.8 Implant swelling

Implants were treated as for the *in vitro* drug release studies. At pre-determined time points, implants were withdrawn and excess water was carefully removed using Kimtech precision wipes (Kimberly-Clark, Rouen, France). Pictures were taken using a SZN-6 trinocular stereo zoom microscope (Optika), equipped with an optical camera (Optika Vison Lite 2.1 software). Furthermore, the implants were weighed [*wet mass (t)*], and the *change in wet mass (%) (t)* was calculated as follows:

$$change\ in\ wet\ mass\ (\%)(t) = \frac{wet\ mass\ (t) - mass\ (t{=}0)}{mass\ (t{=}0)} \times 100\ \% \qquad (1)$$

where *mass (t = 0)* denotes the implant's mass before exposure to the release medium. All experiments were conducted in triplicate. Mean values +/- standard deviations are reported.

2.9 Implant erosion and PLGA degradation

Implants were treated as for the *in vitro* drug release studies. At pre-determined time points, implant samples were withdrawn and freeze dried (freezing at -45°C for 2 h 35 min, primary drying at -20 °C/0.940 mbar for 35 h 10 min, secondary drying at +20 °C/0.0050 mbar for 35 h; Christ Alpha 2-4 LSC+; Martin Christ, Osterode, Germany).

The lyophilizates were weighed [*dry mass (t)*], and the *dry mass (%) (t)* was calculated as follows:

$$dry\ mass\ (\%)(t) = \frac{dry\ mass\ (t)}{mass\ (t{=}0)} \times 100\ \% \qquad (2)$$

where *mass (t = 0)* denotes the implant's mass before exposure to the release medium. All experiments were conducted in triplicate. Mean values +/- standard deviations are reported.

In addition, the average polymer molecular weight (Mw) of the PLGA in the lyophilizates was determined by gel permeation chromatography (GPC) as described in *section 2.6 Gel permeation chromatography (GPC).*

All experiments were conducted in triplicate. Mean values +/- standard deviations are reported.

2.10 Scanning electron microscopy (SEM)

The internal and external morphology of the implants before and after exposure to the release medium was studied using a JEOL Field Emission Scanning Electron Microscope (JSM-7800F, Japan), equipped with the Aztec 3.3 software (Oxford Instruments, Oxfordshire, England). Samples were fixed with a ribbon carbon double-sided adhesive and covered with a fine chrome layer. In the case of implants, which had been exposed to the release medium, the

systems were treated as described for the *in vitro* release studies. At predetermined time points, implant samples were withdrawn, optionally cut using a scalpel (for cross sections) and freeze-dried (as described in *section 2.9*): Thus, caution must be paid to artefact creation during sample preparation.

3. Results and discussion

3.1 Implant properties before exposure to the release media

Figure 3 shows optical microscopy pictures of the 3D printed, ibuprofen-loaded implants with varying theoretical filling density before exposure to the release media. The degree of magnification increases from the top to the bottom. The *theoretical* filling density indicates the theoretical portion of drug-polymer filaments in the implant. For example, an implant with a filling density of 10 % theoretically consists of 10 % drug-polymer filaments and 90 % voids. As it can be seen in Figure 3, the *practical* filling densities were higher. This is because the ibuprofen-PLGA droplets, which were deposited during 3D printing, did not fuse together to form *straight* filaments, but *curved* ones. They, thus, partially filled the voids.

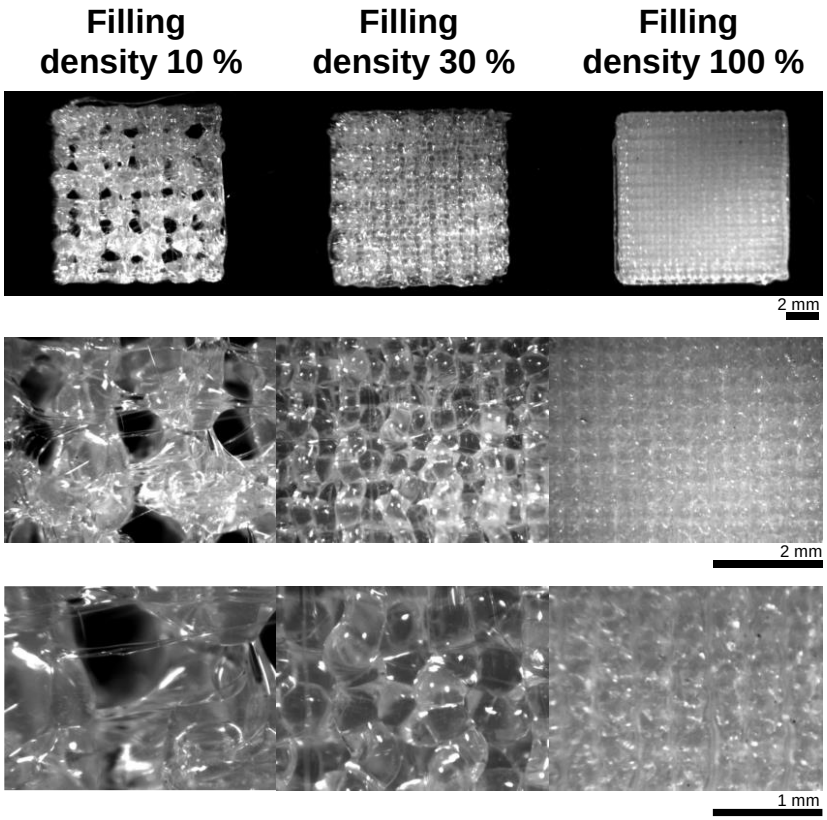

Figure 3: Optical macroscopy pictures of surfaces of ibuprofen-loaded PLGA implants prepared by 3D printing before exposure to the release medium. The theoretical filling density was varied from 10 to 100 %, as indicated.

Table 1 shows the dimensions, mesh pore sizes, practical loadings, glass transition temperatures (Tgs) and average polymer molecular weights (Mw) of the PLGA in the implants before exposure to the release media. As it can be seen, the weight of the implants increased with increasing filling density. This is because the outer implant dimensions were kept constant in this study (approximately 10 x 10 x 2.5 mm), and the portion of the voids decreased with increasing filling density. The practical drug loading was about the same for all implants: 13-14 % (w/w). Also the glass transition temperatures (Tgs) of the PLGA in the implants were similar: about 34-35 °C (DSC thermograms are shown in Figure S2). This is consistent with an about constant polymer molecular weight (Mw) of approximately 15-17 kDa (note the

relatively high standard deviation for implants with 100 % filling density). The PLGA raw material and drug-loaded pellets (used as intermediate product to feed the 3D printer), exhibited polymer molecular weights of 27.7 ± 0.2 kDa and 25.7 ± 0.1 kDa, respectively. Thus, the PLGA chain length decreased during hot melt extrusion and 3D printing because of the exposure to heat and shear forces.

Table 1: Key properties of the 3D printed PLGA implants before exposure to the release media (Tg: glass transition temperature, Mw: average polymer molecular weight). Mean values ± standard deviations are indicated (n = 36 for weight, length, width, mesh pore size; n = 6 for practical drug loading; n = 3 for Tg and Mw).

Theoretical filling density	**10 %**	**30 %**	**100 %**
Weight (mg)	206.5 ± 5.9	212.1 ± 8.4	304.7 ± 11.1
Length – width (mm)	10.4 ± 0.4	10.4 ± 0.2	10.0 ± 0.1
Mesh pore size (mm)	1.1 ± 0.2	0.5 ± 0.1	-
Practical drug loading (%)	13.6 ± 0.2	13.8 ± 0.1	13.4 ± 0.1
Practical drug loading (mg)	28.1 ± 0.8	29.3 ± 1.2	40.8 ± 1.5
Tg (°C)	33.7 ± 0.3	34.6 ± 0.1	34.0 ± 0.8
Mw (kDa)	16.7 ± 0.5	15.8 ± 0.3	15.0 ± 2.0

The DSC thermogram of the ibuprofen raw material showed a clear melting peak at 79.9 ± 0.1°C (Figure S2), indicating that the drug was initially in the crystalline state. In contrast, the DSC thermograms of the different types of implants, as well as the DSC thermogram of the pellets did not show evidence for the presence of important amounts of crystalline ibuprofen. This is consistent with previous studies, reporting that the solubility of ibuprofen in this polymer is at least 10 % [47]. Thus, most of the drug was likely *dissolved* in the polymeric matrix. This is in good agreement with the SEM pictures of surfaces and cross sections of the 3D printed implants before exposure to the release medium (Figure 4): No signs for the presence of noteworthy amounts of drug particles were visible. At higher magnification, numerous tiny pores can be seen in the cross sections, irrespective of the filling density. This can likely be attributed to the evaporation of water and/or ibuprofen during pressing at elevated temperatures and shear forces [36].

The glass transition temperature of the PLGA raw material was 47.2 +/ 0.1 °C (Figure S2). This compares to about 34-35 °C for the implants (Table 1). The decrease can be explained by the decrease in polymer molecular weight (Table 1) and to the plasticizing effect of ibuprofen for PLGA: It has recently been shown that adding increasing amounts of ibuprofen to PLGA 503H led to a decrease in the glass transition temperature of the system, before leveling off and reaching a plateau value [47].

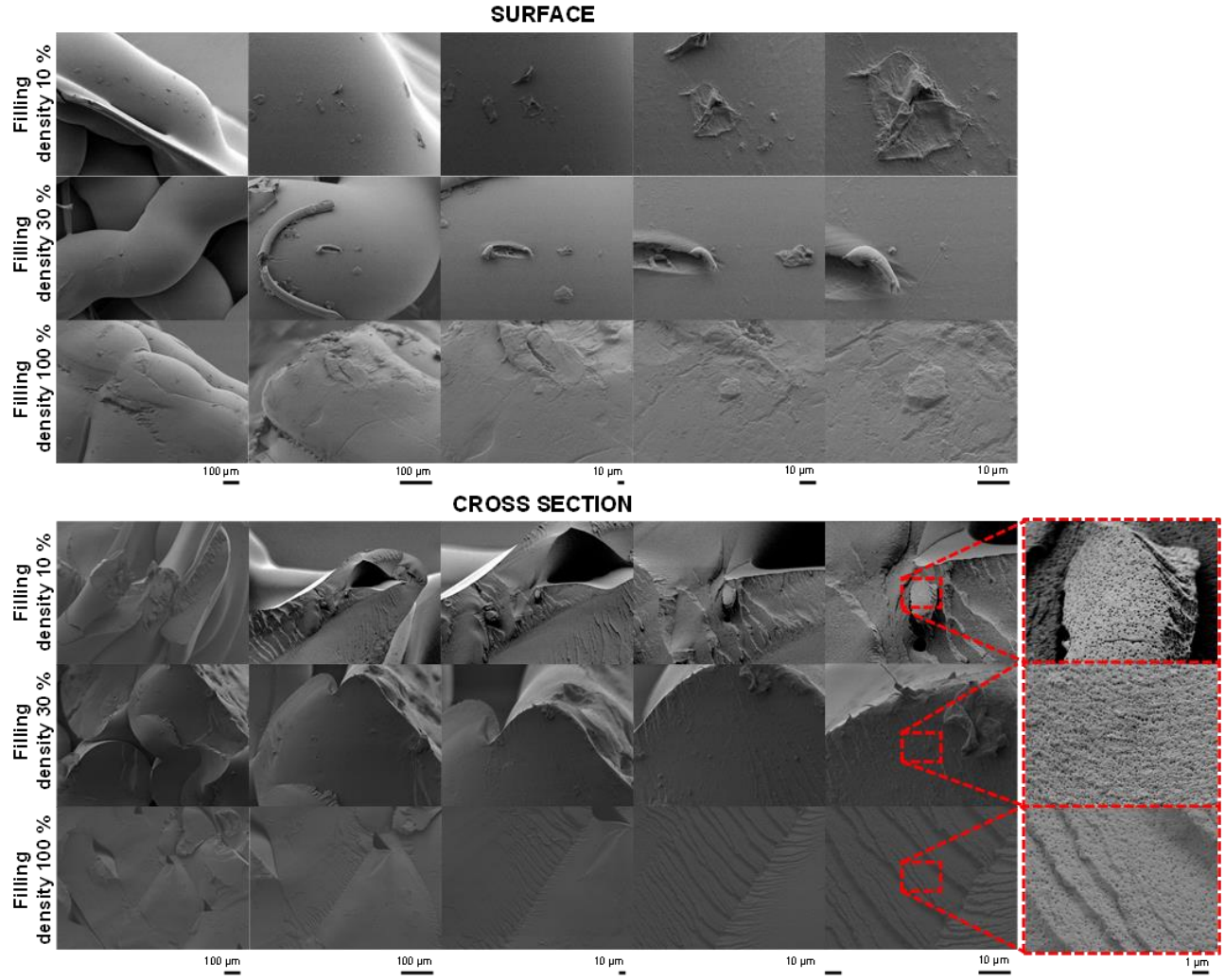

Figure 4: SEM pictures of surfaces and cross sections of the 3D printed, ibuprofen-loaded PLGA implants before exposure to the release medium. The theoretical filling density was varied from 10 to 100 %, as indicated. The red rectangles highlight zones viewed at different degrees of magnification.

3.2 Drug release kinetics

Figure 5 shows the experimentally measured ibuprofen release kinetics from the 3D printed PLGA implants with a theoretical filling density of 10, 30 and 100 %, respectively. On the left hand side, drug release into agarose gels is illustrated, on the right hand side drug release into well agitated phosphate buffer pH 7.4. The experimental set-ups illustrated in Figure 2 were used.

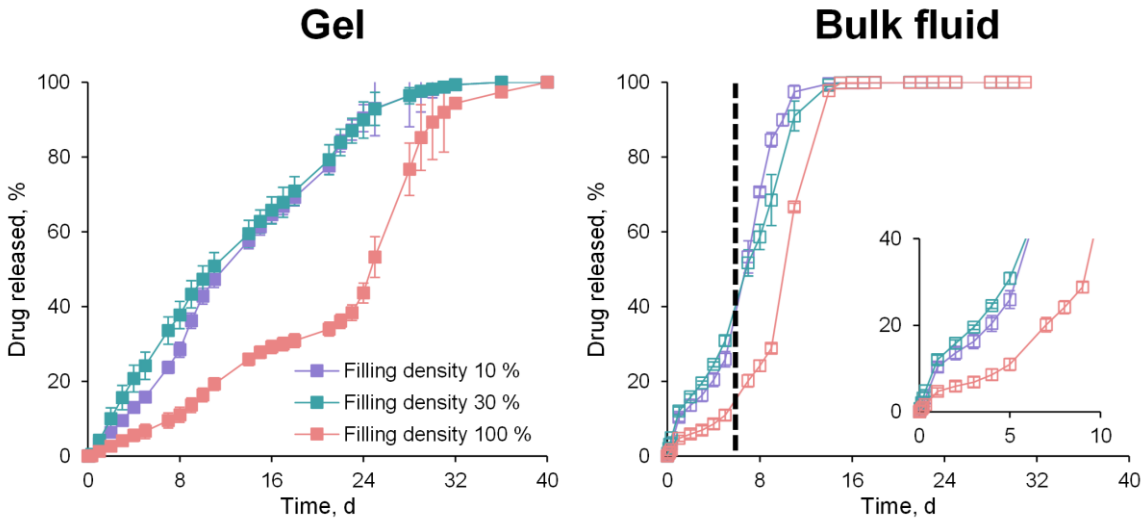

Figure 5: Ibuprofen release kinetics from the investigated, 3D printed PLGA implants into agarose gels and well agitated phosphate buffer pH 7.4 bulk fluid (the experimental set-ups are shown in Figure 2) (n = 3, mean values +/- SD).

Importantly, the resulting drug release kinetics were similar for implants with 10 and 30 % filling density, but substantially different from implants with 100 % filling density, irrespective of the experimental release set-up used: gel or bulk fluid. In both cases, ibuprofen release was more delayed at 100 % filling density. In addition, the *shape* of the release profile from implants with 100 % filling density was different compared to 10 and 30 % filling density in the agarose gel set-up. In contrast, upon implant exposure to the well agitated bulk fluid (phosphate buffer pH 7.4), similar shapes were observed for all filling densities (Figure 5, right hand side): Three drug release phases could be distinguished: (i) A limited burst release during the first day, followed by (ii) an about "zero order" drug release phase (with an approximately constant drug release rate), and (iii) a final, again, more rapid drug release phase, leading to complete drug exhaust. Upon implant exposure to the agarose gel, the observed burst release was negligible. But please note that this is in great part due to a technical limitation of this release set-up: The sampling medium was not the agarose gel itself, but the bulk fluid, which was in contact with the agarose gel (Figure 2). This very much reduces the practical workload during the drug release measurements, but introduces an error: Not the entire amount of drug, which has been released from the implant, is immediately detected. A portion of it is diffusing through the agarose gel at the sampling time point, remaining "undetected". It has previously been shown that the introduced error is generally negligible, because drug diffusion through the gel is fast compared to drug release from the implants [43]. However, if the amounts of released drug are very small and the considered time periods are short (e.g., limited burst release within the 1st day), the introduced error can be *relatively* important. Interestingly, only the implants with a filling density of 100 % clearly showed a final rapid drug release phase in the agarose gel, but not the systems with 10 or 30 % filling density (Figures 5). The latter exhibited an about constant drug release rate throughout the entire release period.

In order to better understand the observed impact of the filling density of the implants as well as of the type of experimental set-up (agarose gels vs. bulk fluids), potential dynamic changes of the key properties of the implants upon exposure to the release media were monitored.

3.3 Dynamic changes in the implants' properties and underlying drug release mechanism

Figure 6A shows the gravimetrically measured variations in the implants' wet mass upon exposure to agarose gels (left hand side) or well agitated phosphate buffer pH 7.4 (right hand side). As it can be seen, the changes were limited within the first few days. But at later time points, substantial system swelling set on. Figure 7 shows optical macroscopy pictures of the implants taken after different exposure times to the release media. Please note that these pictures could be taken during a longer time period compared to the wet mass measurements in Figure 6 (the polymer gels became too fragile for handling & weighing at later time points). As it can be seen in Figure 6A (right hand side) and Figure 7 (bottom), substantial implant swelling set on after about 6 d exposure to well agitated phosphate buffer pH 7.4. This coincided with the onset of the final rapid drug release phase from these systems (Figure 5, right hand side). In contrast, the beginning of important system swelling was delayed, when the implants were imbedded into agarose gels (Figure 7). This can be attributed to the mechanical constraint caused by the presence of the gel [43]. Implants with 10 and 30 % filling density started to significantly swell after about 15-18 d, whereas implants with 100 % filling density started substantial swelling after approximately 21-25 d (Figure 7). Again, the onset of fundamental system swelling coincided well with the onset of the final rapid drug release phase for implants with 100 % filling density (Figure 5). In the case of implants with 10 and 30 % filling density, most of the drug was already released from the implants at this time point.

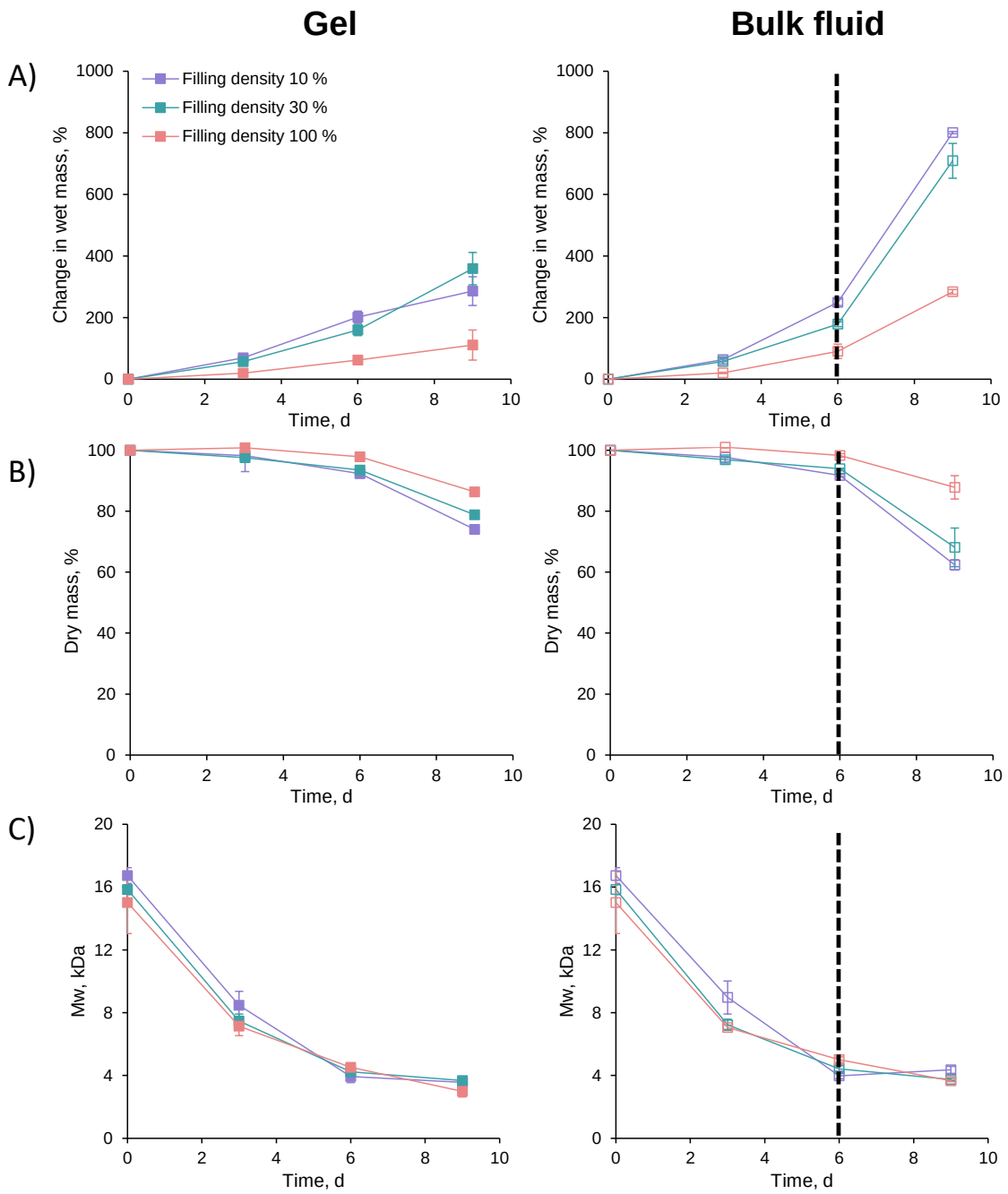

Figure 6: Dynamic changes in the A) wet mass (%), B) dry mass (%), and C) PLGA polymer molecular weight (Mw) of the implants upon exposure to agarose gels (left hand side) or well agitated phosphate buffer pH 7.4 (right hand side) (the experimental set-ups are shown in Figure 2) (n = 3, mean values +/- SD).

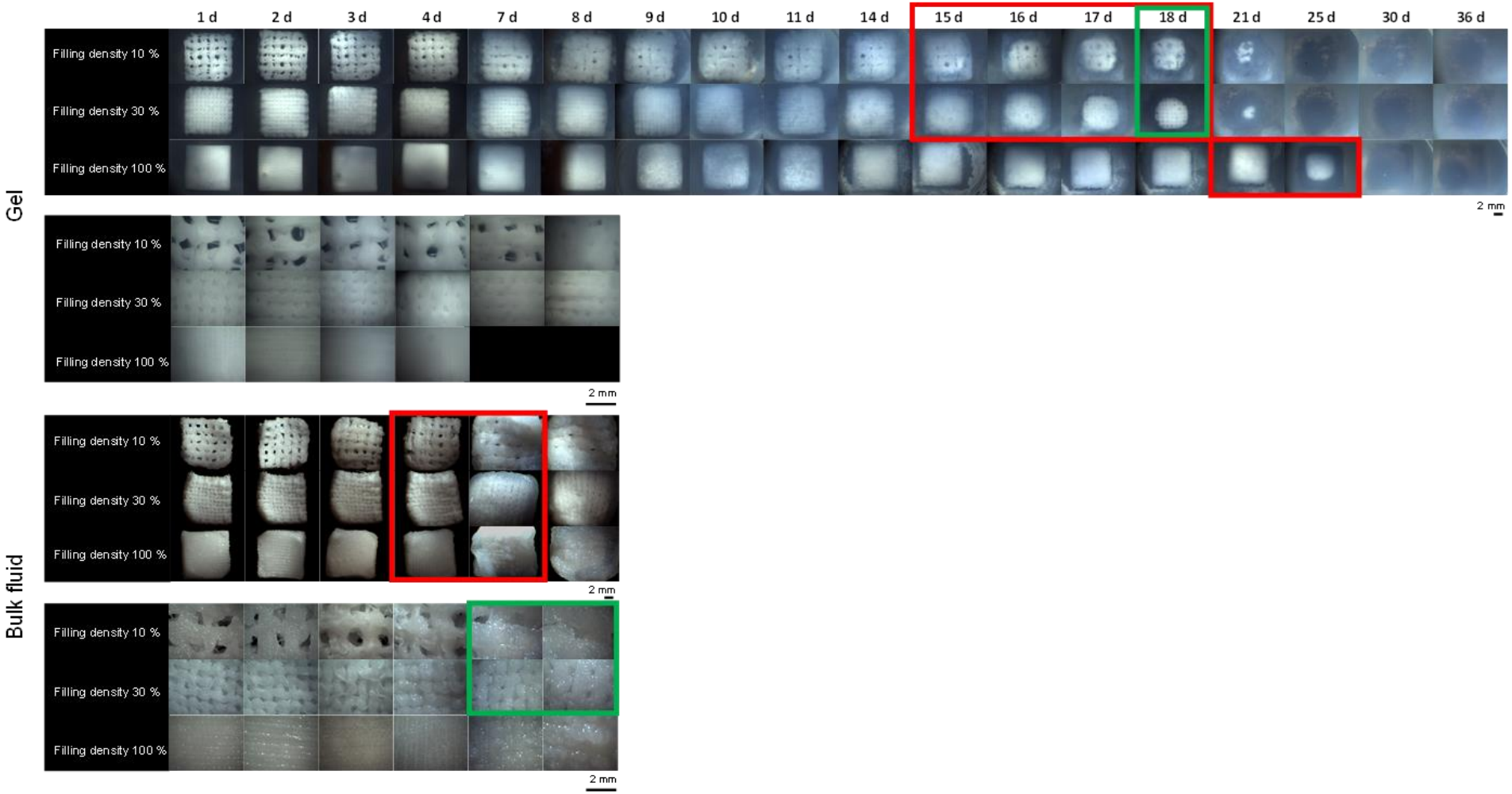

Figure 7: Optical macroscopy pictures of surfaces of the investigated 3D printed implants after exposure to agarose gels (top) or well agitated phosphate buffer pH 7.4 (bottom) (the experimental set-ups are shown in Figure 2). The red rectangles highlight periods in which substantial system swelling set on. The green rectangles highlight the existence of voids in implants with 10 or 30 % filling density, even at late time points.

These observations are consistent with the hypothesis that polymer swelling plays an "orchestrating" role for the control of drug release from PLGA-based delivery systems [30,31,43]. Initially, the polymeric implants are rather hydrophobic and only limited amounts of water can diffuse into the systems. However, these limited water amounts wet the entire devices and polyester bond cleave starts throughout the systems ("bulk degradation") (Figure 8). With time, the polymer chains become shorter and less entangled. Thus, the mechanical stability of the polymeric matrices decreases. Importantly, each ester bond cleavage creates 2 new *hydrophilic* end groups: a -COOH and an -OH end group (illustrated as blue dots in the scheme in Figure 8). Consequently, the system also becomes more and more hydrophilic. In addition, water soluble degradation products are generated, creating a steadily increasing osmotic pressure, attracting water into the system. At a certain time point, the implants are sufficiently hydrophilic, mechanically weak and exhibit a non-negligible osmotic pressure so that large amounts of water penetrate into the implants: *substantial* implant swelling sets on. This results in much higher drug mobility and, hence, increased drug release rates, explaining the final rapid drug release phases, leading to complete drug exhaust.

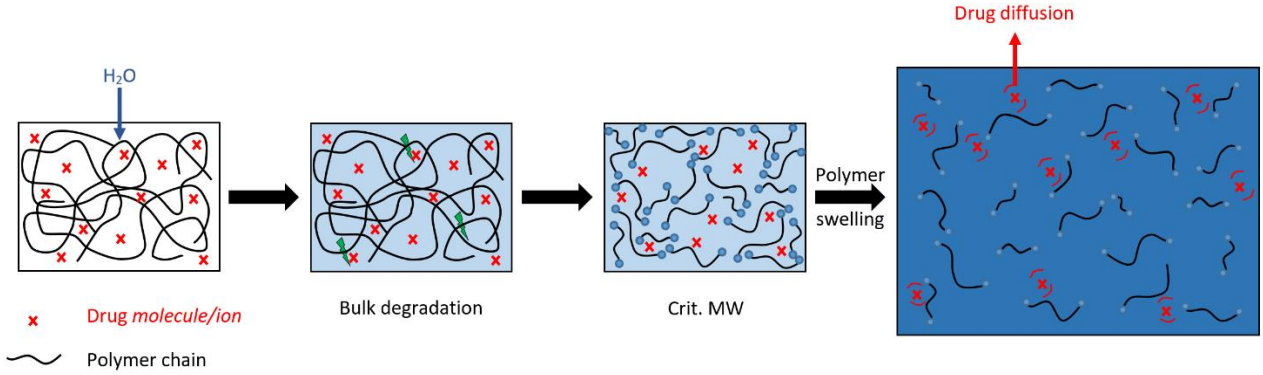

Figure 8: Schematic presentation of underlying drug release mechanism from the investigated implants. The crosses represent individual drug molecules/ions. Details are described in the text.

This drug release mechanism seems to govern also the 3D printed implants in the present study: Upon exposure to *well agitated phosphate buffer*, it takes about 6 d for the devices to reach a certain, critical polymer molecular weight (Figure 6C). At this point, substantial implant swelling sets on, coinciding with the onset of the final rapid drug release phases (Figure 5, right hand side). In addition to the drug, also water soluble polymer degradation products become more mobile and diffuse out of the system. Both, ibuprofen and degradation product leaching result in the onset of noteworthy dry mass loss (Figure 6B). Importantly, the presence of the agarose gel physically hinders implant swelling (Figures 6A and 7) and, thus, delays the onset of the final rapid drug release phases (Figure 5, left hand side). In vivo, the presence of human tissue around the implant can be expected to exhibit a similar mechanical effect.

It has to be pointed out that the experimental set-up (agarose gel vs. well agitated phosphate buffer) and filling density did not affect the *polymer degradation* kinetics to a noteworthy extent (Figure 6C): The PLGA polymer molecular weight decreased in a similar manner in all cases. This is sound, because all implants are rapidly entirely wetted upon exposure to the release media, and ester bond cleavage starts at about the same time throughout all devices. The fact that these similar *polymer degradation* kinetics (Figure 6C) do not lead to similar *drug release* kinetics from the implants (Figure 5) indicates that *PLGA degradation* does not seem to play an orchestrating role for the control of drug release. Instead, polymer swelling seems to dominate.

The SEM pictures in Figure 9 show the morphology of surfaces and cross sections of the 3D printed implants after 3 d exposure to the release media: agarose gels (top) and well agitated phosphate buffer (bottom). Please note that great caution must be paid due to artefact creation, because the implants were freeze dried prior to analysis. As it can be seen, all surfaces are highly shriveled. During drug release these regions are highly swollen gels (optical macroscopy pictures in Figure 7). Upon lyophilization, the water is removed and the structures collapse. Importantly, the cross sections in Figure 9 show that only surface near regions were substantially swollen at this time point, whereas the inner implant zones were not. This is because the surfaces are exposed to 100 % water from the beginning. In contrast, the amounts of water present *within* the polymeric systems are limited at early time points. Consequently, PLGA degradation occurs much more rapid in surface near regions. This rapidly occuring *locally restricted* swelling of surface near regions must not be confused with the substantial swelling of the *entire* implants occurring at later time points (illustrated on the right hand side in Figure 8).

The fact that the observed ibuprofen release kinetics were similar from implants with 10 and 30 % filling density, but slower from implants with 100 % filling density (irrespective of the type of experimental set-up), can probably be explained as follows: In an implant with 10 or 30 % filling density, it is sufficient for the drug to diffuse out of a *single filament* in order to be released. This is schematically illustrated in the cartoon in Figure 10. A red cross represents an individual ibuprofen molecule or ion. Once released from a filament within the implant mesh, the drug is located in water filled voids, which are interconnected. Mass transport in this continuous aqueous phase can be expected to be much more rapid than drug transport in the polymeric phase. These voids exist even at late time points, as indicated by the green rectangles in Figure 7. In contrast, in implants with 100 % filling density the diffusion pathways through the polymeric matrix to be overcome by the drug are much longer (Figure 10): The *ensemble of polymer filaments* acts as a more or less homogeneous continuum for drug diffusion: If a drug molecule/ion is released from a filament located deeper within the mesh, it is not yet released into the surrounding medium (bulk fluid or agarose gel). It must subsequently diffuse through other filaments and/or find its way through the tiny spaces between filaments, which are filled with swollen PLGA gel (surface near regions are exposed to 100 % water and rather rapidly swell, please see discussion above).

Note that once the *entire* system has undergone substantial swelling (e.g. after about 6 d in the bulk fluid set-up), a more or less homogeneous “PLGA gel” is formed in all cases. Drug release from these highly swollen polymer gels is relatively rapid, irrespective of the initial filling density (Figure 5).

It has to be highlighted that the impact of the filling density of the 3D printed implants on drug release is much more pronounced in the agarose set-up compared to the well agitated bulk fluid set-up (Figure 5 left *vs.* right hand side). This is likely also of practical importance: The tissue surrounding the implants upon administration to a patient can be expected to limit polymer swelling (as the agarose gel does in this study). Since polymer swelling plays an “orchestrating” role for drug release, this has non-negligible consequences.

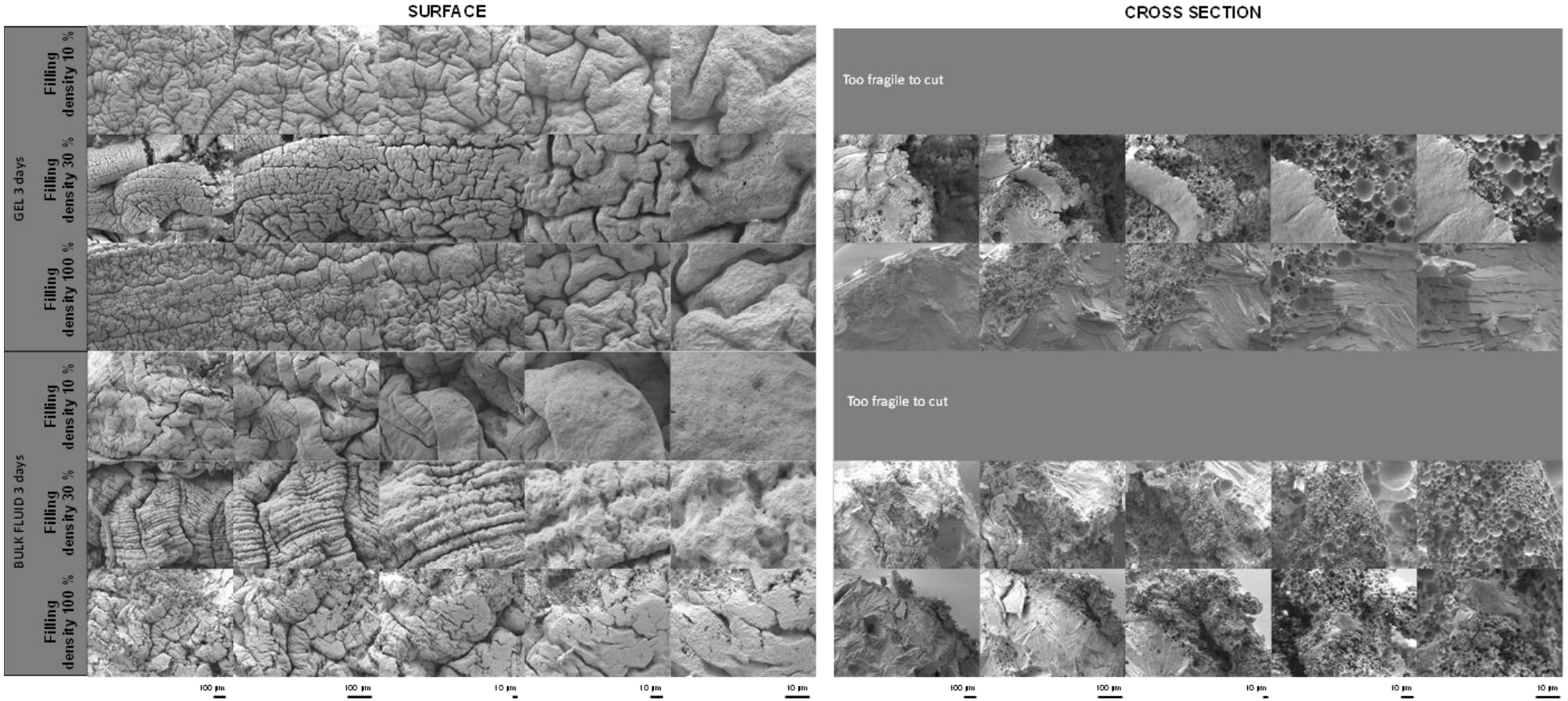

Figure 9: SEM pictures of surfaces and cross sections of the investigated PLGA implants after 3 days exposure to agarose gels (top) or well agitated phosphate buffer pH 7.4 (bottom) (the experimental set-ups are shown in Figure 2). Please note that the implants were freeze-dried prior to analysis. Thus, caution must be paid due to artefact creation.

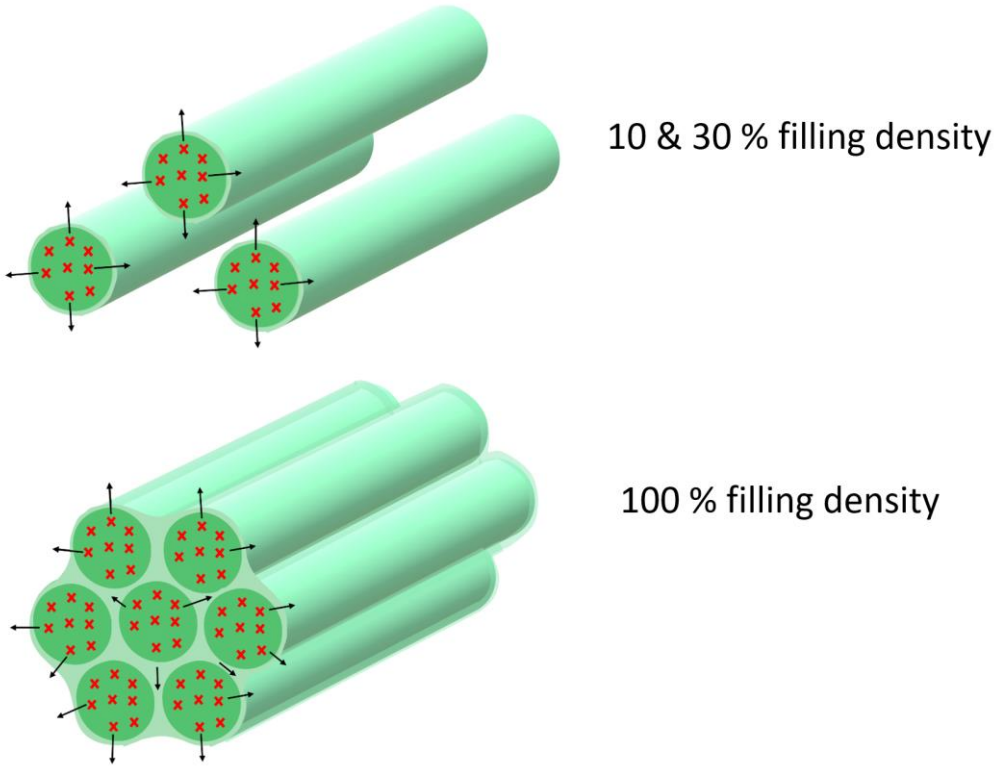

Figure 10: Schematic presentation of drug release from implants with varying filling density. The red crosses represent individual drug molecules/ions.

4. Conclusion

The filling density of 3D printed PLGA implants can fundamentally affect the diffusion pathways for the drug: As long as a continuous aqueous phase exists between the polymer filaments, the drug diffusion pathways through the macromolecular networks are relatively short: at the maximum the radius of a *single filament*. However, if the filling density is sufficiently high and no interconnected network of water-filled channels exists, the drug must diffuse through a more or less homogeneous PLGA phase with the dimension of the *entire* implant. This can significantly slow down drug release.

In addition, the "orchestrating role" of substantial system swelling for the control of drug release was confirmed in the present study as well as the importance of the presence of an outer gel phase: Ibuprofen release was much slower into agarose gels compared to well agitated phosphate buffer, because system swelling was mechanically hindered and delayed. In vivo, living tissue can also be expected to hinder implant swelling. In contrast, the *polymer degradation* kinetics were similar for all the investigated cases and could not explain the observed differences in drug release.

This mechanistic understanding of the control of drug release from PLGA-based delivery systems can be expected to facilitate the optimization of this type of devices and speed up drug product development.

Acknowledgements

This project has received funding from the Interreg 2 Seas programme 2014-2020 co-funded by the European Regional Development Fund under subsidy contracts No 2S04-014 3DMed and 2S07-033 Site Drug.

References

1 Park H and Otte A, Park K. Evolution of drug delivery systems: From 1950 to 2020 and beyond. J Control Release 342 (2022) 53-65.

2 Arrighi A, Marquette S, Peerboom C et al. Development of PLGA microparticles with high immunoglobulin G-loaded levels and sustained-release properties obtained by spray-drying a water-in-oil emulsion, Int J Pharmaceut 566 (2019) 291–298.

3 Parent M, Clarot I, Gibot S et al. One-week in vivo sustained release of a peptide formulated into in situ forming implants, Int J Pharmaceut 521 (2017) 357–360.

4 Sato Y, Moritani T, Inoue R et al. Preparation and evaluation of sustained release formulation of PLGA using a new injection system based on ink-jet injection technology. Int J Pharmaceut 635 (2023) 122731.

5 Bassand C, Benabed L, Freitag J et al. How bulk fluid renewal can affect in vitro drug release from PLGA implants: Importance of the experimental set-up. Int J Pharmaceut: X 4 (2022) 1-10, 100131.

6 Anderson J and Shives M. Biodegradation and biocompatibility of PLA and PLGA microspheres. Adv Drug Deliv Rev 28 (1997) 5–24.

7 Luan X and Bodmeier R. Modification of the tri-phasic drug release pattern of leuprolide acetate-loaded poly(lactide-co-glycolide) microparticles. Eur J Pharm Biopharm 63 (2006) 205–214.

8 Shi NQ, Zhou J, Walker J et al. Microencapsulation of luteinizing hormone-releasing hormone agonist in poly (lactic-co-glycolic acid) microspheres by spray-drying. J Control Release 321 (2020) 756–772.

9 Acharya G, Shin CS, Vedantham K et al. A study of drug release from homogeneous PLGA microstructures, J Control Release. 146 (2010) 201–206.

10 Mylonaki I, Allemann E, Delie F et al. Imaging the porous structure in the core of degrading PLGA microparticles: The effect of molecular weight, J Control Release 286 (2018) 231–239.

11 Chen W, Palazzo A, Hennink WE et al. Effect of Particle Size on Drug Loading and Release Kinetics of Gefitinib-Loaded PLGA Microspheres. Mol Pharm 14 (2017) 459–67.

12 Wischke C and Schwendeman SP. Principles of encapsulating hydrophobic drugs in PLA/PLGA microparticles, Int J Pharmaceut 364 (2008) 298–327.

13 Ramazani F, Chen W, van Nostrum CF et al. Strategies for encapsulation of small hydrophilic and amphiphilic drugs in PLGA microspheres: State-of-the-art and challenges, Int J Pharmaceut 499 (2016) 358–367.

14 Park K, Skidmore S, Hadar J et al. Injectable, long-acting PLGA formulations: Analyzing PLGA and understanding microparticle formation. J Control Release 304 (2019) 125-134.

15 Jain A, Kunduru KR, Basu A et al. Injectable formulations of poly(lactic acid) and its copolymers in clinical use. Adv Drug Deliv Rev 107 (2016) 213–227.

16 Siepmann J, Elkharraz K, Siepmann F et al. How autocatalysis accelerates drug release from PLGA-based microparticles: a quantitative treatment. Biomacromolecules 6 (2005) 2312-2319.

17 Klose D, Siepmann F, Elkharraz K et al. How porosity and size affect the drug release mechanisms from PLGA-based microparticles. Int J Pharmaceut 314 (2006) 198-206.

18 Goepferich, A. Mechanisms of polymer degradation and erosion. Biomaterials 17 (1996) 103–114.

19 Fredenberg S, Wahlgren M, Reslow M et al. The mechanisms of drug release in poly(lactic-co-glycolic acid)-based drug delivery systems--a review. Int J Pharmaceut 415 (2011) 34–52.

20 Wang J, Wang BM, Schwendeman SP. Characterization of the initial burst release of a model peptide from poly(D,L-lactide-co-glycolide) microspheres. J Control Release 82 (2002) 289–307.

21 Fredenberg S, Joensson M, Laakso T et al. Development of mass transport resistance in poly(lactide-co-glycolide) films and particles – A mechanistic study. Int J Pharmaceut 409 (2011) 194–202.

22 Huang, J, Mazzara, JM, Schwendeman, SP et al. Self-healing of pores in PLGAs. J Control Release 206 (2015) 20–29.

23 Quan P, Guo W, Yang L et al. Donepezil accelerates the release of PLGA microparticles via catalyzing the polymer degradation regardless of the end groups and molecular weights. Int J Pharmaceut 632 (2023) 122566.

24 von Burkersroda F, Schedl L and Goepferich A. Why degradable polymers undergo surface erosion or bulk erosion. Biomaterials 23 (2002) 4221–4231.

25 Blasi P, Schoubben A, Giovagnoli S et al. Ketoprofen poly(lactide-co-glycolide) physical interaction. AAPS Pharm Sci Tech 8 (2007) E78–E85.

26 Schaedlich, A, Kempe, S, Maeder K. Non-invasive in vivo characterization of microclimate pH inside in situ forming PLGA implants using multispectral fluorescence imaging. J Control Release 179 (2014) 52-62.

27 Fu, K, Pack, DW, Klibanov, AM et al. Visual Evidence of Acidic Environment Within Degrading Poly(lactic-co-glycolic acid) (PLGA) Microspheres. Pharm Res 17 (2000) 100–106.

28 Brunner, A, Maeder K, Goepferich, A. pH and osmotic pressure inside biodegradable microspheres during erosion. Pharm Res 16 (1999) 847–853.

29 Hong JKY, Schutzman R, Olsen K et al. Mapping in vivo microclimate pH distribution in exenatide-encapsulated PLGA microspheres. J Control Release 352 (2022) 438–449.

30 Gasmi H, Danede F, Siepmann J et al. Does PLGA microparticle swelling control drug release? New insight based on single particle swelling studies. J Control Release 213, 120-127, 2015.

31 Bode C, Kranz H, Fivez A et al. Often neglected: PLGA/PLA swelling orchestrates drug release - HME implants. J Control Release 306, 97-107, 2019.

32 Maturavongsadit P, Paravyan G, Kovarova M et al. A new engineering process of biodegradable polymeric solid implants for ultra-long-acting drug delivery. biodegradable polymeric solid implants for ultra-long-acting drug delivery. Int J Pharmaceut: X 3 (2021), 100068.

33 Lehner A, Liebau K, Syrowatka et al. Novel biodegradable Round Window Disks for inner ear delivery of dexamethasone. Int J Pharmaceut 594 (2020) 120180.

34 Cosse A, Koenig C, Lamprecht A et al. Hot Melt Extrusion for Sustained Protein Release: Matrix Erosion and In Vitro Release of PLGA-Based Implants. AAPS Pharm Sci Tech 18 (2017) 15-26.

35 Serris I, Serris P, Frey KM et al. Development of 3D-Printed Layered PLGA Films for Drug Delivery and Evaluation of Drug Release Behaviors. AAPS Pharm Sci Tech. 21 (2020) https://doi.org/10.1208/s12249-020-01790-1.

36 Bassand C, Benabed L, Charlon S et al. 3D Printed PLGA implants: APF DDM vs. FDM. J Control Release 353, 864–874, 2023.

37 Maroni A, Melocchi A, Parietti F et al. 3D printed multi-compartment capsular devices for two-pulse oral drug delivery. J Control Release 268 (2017) 10-18.

38 Ragelle H, Rahimian S, Guzzi EA et al. Additive manufacturing in drug delivery: Innovative drug product design and opportunities for industrial application. Adv Drug Deliv Rev. 178 (2021) 113990.

39 Seoane-Viano I, Januskaite P, Alvarez Lorenzo C et al. Semi-solid extrusion 3D printing in drug delivery and biomedicine: Personalised solutions for healthcare challenges. J Control Release 332 (2021) 367-389.
40 Awad A, Fina F, Goyanes A et al. Advances in powder bed fusion 3D printing in drug delivery and healthcare. Adv Drug Deliv Rev 174 (2021) 406-424.
41 Diaz-Torres E, Rodríguez-Pombo L, Jie Ong J et al. Integrating pressure sensor control into semi-solid extrusion 3D printing to optimize medicine manufacturing. Int J Pharmaceut: X 4 (2022) 100133.
42 Ye F, Larsen SW, Yaghmur A et al. Drug release into hydrogel-based subcutaneous surrogates studied by UV imaging, J. Pharm. Biomed. Anal. 71 (2012) 27–34.
43 Bassand C, Verin J, Lamatsch M et al. How agarose gels surrounding PLGA implants limit swelling and slow down drug release. J Control Release 343 (2022) 255-266.
44 Kozak J, Rabiskova M, Lamprecht A. In-vitro drug release testing of parenteral formulations via an agarose gel envelope to closer mimic tissue firmness. Int J Pharmaceut. 594 (2021) 120142.
45 Kraibuhler H, Duffner E. Device for the production of a three-dimensional object. US20140113017A1 (2018) 9889604.
46 Kraibuhler H, Duffner E, Kessling O. Method for producing a three-dimensional object by means of generative construction. Patent 20160009026 (2018) 10040249.
47 Bassand C, Benabed L, Verin J et al. Hot melt extruded PLGA implants loaded with ibuprofen: how heat exposure alters the physical drug state, J Drug Dev Sci Tech 73 (2022) 103432.